
COMBINING STRAIGHT-LINE AND MAP-BASED DISTANCES TO INVESTIGATE THE CONNECTION BETWEEN PROXIMITY TO HEALTHY FOODS AND DISEASE

A PREPRINT

✉ **Sarah C. Lotspeich**
Department of Statistical Sciences
Wake Forest University
Winston-Salem, NC 27109
lotspes@wfu.edu

Ashley E. Mullan
Department of Statistical Sciences
Wake Forest University
Winston-Salem, NC 27109
mulla22@wfu.edu

Lucy D’Agostino McGowan
Department of Statistical Sciences
Wake Forest University
Winston-Salem, NC 27109
mcgowald@wfu.edu

Staci A. Hepler
Department of Statistical Sciences
Wake Forest University
Winston-Salem, NC 27109
heplersa@wfu.edu

May 28, 2024

ABSTRACT

Healthy foods are essential for a healthy life, but accessing healthy food can be more challenging for some people than others. This disparity in food access may lead to disparities in well-being, potentially with disproportionate rates of diseases in communities that face more challenges in accessing healthy food (i.e., low-access communities). Identifying low-access, high-risk communities for targeted interventions is a public health priority, but current methods to quantify food access rely on distance measures that are either computationally simple (like the length of the shortest straight-line route) or accurate (like the length of the shortest map-based driving route), but not both. We propose a multiple imputation approach to combine these distance measures, allowing researchers to harness the computational ease of one with the accuracy of the other. The approach incorporates straight-line distances for all neighborhoods and map-based distances for just a subset, offering comparable estimates to the “gold standard” model using map-based distances for all neighborhoods and improved efficiency over the “complete case” model using map-based distances for just the subset. Through the adoption of a measurement error framework, information from the straight-line distances can be leveraged to compute informative placeholders (i.e., impute) for any neighborhoods without map-based distances. Using simulations and data for the Piedmont Triad region of North Carolina, we quantify and compare the associations between various health outcomes (diabetes and obesity) and neighborhood-level proximity to healthy foods. The imputation procedure also makes it possible to predict the full landscape of food access in an area without requiring map-based measurements for all neighborhoods.

Keywords Census tract · Diabetes · Google Maps · Haversine formula · Measurement error · Missing data · Network distance · Obesity · SNAP

1 Motivation

Eating healthy foods is critical to childhood development and preventing illnesses in adulthood, including diabetes and obesity [Liu et al., 2000, Harding et al., 2008]. However, eating healthy foods is not just a choice; having access

to healthy food options also determines what people eat. For some people, predominantly those with disabilities and in low-income or minority communities, healthy foods are not always accessible [Bower et al., 2014, Brucker and Coleman-Jensen, 2017]. Access can be hampered by physical factors, like geographic proximity and the availability of public transit [Bennion et al., 2022], and social factors, like structural racism and discrimination [Burke et al., 2018, Odoms-Young and Bruce, 2018]. Thus, not just consumption of healthy foods but access to them can impact health [Ahern et al., 2011, Gallegos et al., 2021, Kanchi et al., 2021, Li et al., 2021], and disparities in access can potentially perpetuate disparities in health [Larson et al., 2009].

For public health officials seeking to reduce the burden of diet-related non-communicable diseases, understanding (i) the landscape of food access in a community and (ii) the disease’s connection to food access can be informative. When helping public health officials understand these issues, quantifying food access is an important place to start. To identify low-access, high-risk neighborhoods, food access can be quantified using (i) *proximity*, i.e., how far away healthy food stores are, or (ii) *density*, i.e., how many healthy food stores are within some radius. Using geocoded store locations, we focus on neighborhood proximity to healthy foods, defined as the minimum distance between a neighborhood’s “population center” (a population-weighted centroid) and a healthy food store, and the connection between proximity to healthy foods and diagnosed diabetes and obesity prevalence.

1.1 Drawbacks of Current Distance Calculations

When calculating distances between neighborhoods and healthy food stores, there currently exists a trade-off between (i) computationally simple methods that are less accurate and (ii) more accurate methods that are computationally complex. Euclidean distance, which draws a straight line along the shortest path between two points (the healthy food store location and the neighborhood’s population center) “as the crow flies” is among the former. A recent systematic review of studies in the United Kingdom found that Euclidean distance and circular “buffers” based on it were the most commonly used methods to quantify food access [Titus et al., 2021]. (Buffers are commonly circular catchment areas of some specified radius, e.g., one Euclidean mile, from a point of interest.) They are prominent in studies of U.S. food access as well [e.g., Peng et al., 2020, Sánchez et al., 2022]. The Haversine formula, which instead draws the shortest possible arc between two points, can offer better accuracy, particularly over long distances, and it is also computationally simple. Still, both of these calculations ignore transportation infrastructure and natural barriers, underestimating proximity to healthy foods and overestimating neighborhood access. These problems could be exacerbated in rural areas with fewer available stores and fewer accessible straight-line routes.

Map-based (or network) distances more accurately quantify neighborhoods’ proximity to healthy foods and more realistically describe the landscape of food access [Bennion et al., 2022], and they can differ substantially from straight-line ones. For the example in Supplemental Figure S1, it can be seen that the estimated driving distance between the historic Reynolda House in Winston-Salem, North Carolina (NC), and a nearby Food Lion grocery store (2.65 miles) was 1.6 times the straight-line distance between them (1.64 miles). Further, the straight-line route in Supplemental Figure S1 cuts through a pond, making it impassible for residents of the Reynolda House.

Improved versions of the food access measures like proximity can be calculated from map-based distances [Sharkey et al., 2009, Matsuzaki et al., 2023]. The Google Maps API is incredibly powerful for calculations like this, and open-source software in the statistical computing language R [R Core Team, 2023] can integrate the API into a statistical workflow [Kahle and Wickham, 2013, Cooley, 2023]. These tools can calculate the map-based travel distances, offering a more accurate snapshot of a neighborhood’s access. Still, making all necessary calculations may not be feasible due to time-intensive computations and monthly limits on free API usage. Even paid options like ArcGIS can quickly become time-intensive, so obtaining map-based distances for entire studies is potentially unrealistic at scale (e.g., to shape policy at the state or national level versus the county).

1.2 Straight-Line Food Access As a Mismeasured Covariate

With fixed resources, researchers must choose between a small-scale, more accurate study or a large-scale, less accurate one. For example, it would be reasonable to obtain map-based distances for all neighborhoods in one city or county but not in the state. Instead, researchers might sacrifice accuracy to broaden the scope of their study, leading to biased estimates and statistical power loss in the downstream analysis [Carroll et al., 2006]. Still, what if accurate, map-based distances can be calculated for some neighborhoods?

The two-phase design [White, 1982], or internal validation study, is commonly used in the measurement error literature [e.g., Giganti et al., 2020, Nab et al., 2021, Lotspeich et al., 2022] and can be applied here. Straight-line distances are collected for all neighborhoods in Phase I. Then, in Phase II, map-based distances are collected for a chosen subset, which can be strategically selected based on any information fully observed in Phase I. For example, Phase II in the Piedmont Triad analysis was chosen via county-stratified random sampling to ensure geographic diversity. Many other

sampling designs are possible, including strategic ones to target different goals (e.g., to minimize the variance of the downstream model estimates).

Straight-line and map-based methods seek to measure the same quantity but take different paths to get there. Thus, assuming that straight-line distance underestimates map-based, a measurement error model is a natural way to relate more and less accurate food access variables derived from these distances (like proximity). Let X and X^* denote a neighborhood’s proximity to healthy foods based on map-based (error-free) and straight-line (error-prone) distances, respectively. The classical measurement error model [Fuller, 1987] is a popular choice: $X^* = X + U$, where the random errors U are assumed to be independent of X . Often, U is assumed to follow a mean-zero normal distribution, but when measuring proximity to healthy foods the straight-line measure X^* systematically underestimates map-based X by some absolute amount, so $U \leq 0$ necessarily and a different distribution is needed. It may also be desirable to model straight-line X^* as systematically underestimating map-based X by some relative factor instead. A multiplicative error model is also possible: $X^* = XW$, where W is once again assumed to be independent of X . Multiplicative measurement error models are not as common as additive ones, and there is no most popular distribution to assume for them. The main consideration in selecting a distribution for W is that $0 \leq W \leq 1$, since $X^* \leq X$. Fortunately, we do not need to specify the measurement error model to use the proposed multiple imputation approach, and the methods work well under either model. In treating the straight-line proximity to healthy foods as an error-prone version of the map-based proximity, a manageable statistical problem replaces an unmanageable computational one.

1.3 Statistical Modeling With a Mismeasured Covariate

First, suppose that the errors in the straight-line distances were ignored. If the X^* were used instead of X to conduct the so-called “naive” analysis of food access and disease prevalence, the model estimates would be biased and inference under-powered [Carroll et al., 2006]. Linear regression estimates will be attenuated [Fuller, 1987], while logistic [Barron, 1977] and Poisson regression [Videk and Wong, 1996] estimates can be attenuated or exaggerated. These results echo intuition: Measurement errors must be addressed and analyses corrected to obtain valid inferences about the relationship between food access and health.

In the two-phase study, X^* is observed for all neighborhoods and X for only the chosen subset. Many statistical methods can be used to analyze the resulting data with no missing X^* but some missing X , and the popular ones fall into two groups: (i) design-based and (ii) model-based estimators. Most methods require at least partial information on the relationship between error-prone and error-free variables, and these two groups are named for how they handle the missing data in X left behind from the validation study. Complete data from the validation study can be leveraged to overcome the missing map-based measures.

Design-based estimators rely primarily on the sampling probabilities describing which neighborhoods were chosen for map-based measurements (i.e., the study design) to overcome the missing data in X . Included in this class are the popular inverse probability weighted (IPW) [Horvitz and Thompson, 1952] and augmented IPW/generalized raking estimators [Deville et al., 1993, Robins et al., 1994, Oh et al., 2021a,b, Amorim et al., 2024]. Generally, design-based estimators offer better robustness than model-based ones, because they make fewer assumptions about the error mechanism.

Model-based estimators place an extra model on the error mechanism (i.e., the distribution of map-based X given straight-line X^*). Imputation, maximum likelihood estimation, and regression calibration are popular members of this class [Carroll et al., 2006]. Replacing missing X values with predictions based on X^* (i.e., imputation) is a promising and popular option because of its ease of implementation and approachability to statisticians and nonstatisticians. So far, multiple imputation has been used to overcome measurement error in binary outcomes [Edwards et al., 2013] or exposures [Cole et al., 2006, Edwards et al., 2015, 2020]; in continuous outcomes and covariates [Shepherd et al., 2012]; and in a mix of categorical, continuous, or time-to-event variables [Giganti et al., 2020, Han et al., 2021, Pelgrims et al., 2023, Amorim et al., 2024]. When assumptions on the error mechanism are correct, model-based estimators can offer better statistical efficiency than design-based ones.

1.4 Overview

A new statistical approach is proposed to (i) accurately quantify food access on a large geographic scale from incomplete data and (ii) efficiently model its impact on health with less computational strain. This multiple imputation framework is easily generalizable, as adopting other outcome models, adding other fully observed covariates, and incorporating spatial autocorrelation are very straightforward. Also, food access for all neighborhoods in a study can be predicted despite only validating a subset of them, providing a more accurate and comprehensive estimate of the food access landscape. The rest of the paper is organized as follows. In Section 2, we describe the distance calculations and

proposed imputation methods. In Sections 3 and 4, the methods are tested in extensive simulations and applied to data on the northwestern region of North Carolina. In Section 5, we discuss our findings and future directions.

2 Methods

2.1 Model and Data

The neighborhood-level rates of various health outcomes will be modeled in the following way. Specifically, census tracts were adopted as the “neighborhood” unit in for the analysis in Section 4, since that was the smallest geographic scale at which the data were available. Let Y be the model outcome, denoting the number of cases in a neighborhood ($Y \in \{0, 1, \dots\}$). This outcome is offset by Pop , denoting the neighborhood population ($Pop \in \{Y, Y + 1, \dots\}$). The neighborhood’s food access will be measured by X , denoting the proximity to healthy foods ($X \in \mathbb{R}^+$) from the population center, or population-weighted centroid [United States Census Bureau, 2021]. “Healthy food stores” are defined in Section 4.2 and can be thought of as grocery stores or other fresh foods sources.

Poisson regression will be used to assess the impact of food access (measured by X) on the neighborhood-level rate of various health outcomes (Y per Pop), adjusting for other fully observed covariates \mathbf{Z} (e.g., rural/urban status):

$$\log\{E_{\beta}(Y|X)\} = \beta_0 + \beta_1 X + \beta_2^T \mathbf{Z} + \log(Pop). \quad (1)$$

The prevalence ratio for food access, $\exp(\beta_1)$, is of primary interest. A prevalence ratio of $\exp(\beta_1) > 1$ indicates that worse proximity (i.e., farther distances to the neighborhood’s nearest healthy food store) is associated with higher prevalence of the health outcome, $\exp(\beta_1) = 1$ indicates that proximity had no impact on prevalence of the health outcome, and $\exp(\beta_1) < 1$ indicates that worse proximity led to lower prevalence of the health outcome. $\exp(\beta_1) > 1$.

2.2 Distance Calculations

Proximity to healthy foods X is derived from the distances between neighborhood population centers and nearby grocery stores, supermarkets, and other fresh food sources. Suppose data are collected on N neighborhoods and M stores in the study area. If D_{ij} denotes the map-based distance between neighborhood center i ($i \in \{1, \dots, N\}$) and healthy food store j ($j \in \{1, \dots, M\}$), then $X_i = \min(D_{i1}, \dots, D_{iM})$ is neighborhood i ’s map-based proximity to healthy foods. Due to the added computational strain of map-based calculations, the straight-line distances are first calculated for all neighborhoods ($i \in \{1, \dots, n\}$) and stores ($j \in \{1, \dots, M\}$) and then used to narrow down combinations (i, j) of the shortest routes to revisit for the map-based distances.

Straight-line distances D_{ij}^* ($i \in \{1, \dots, N\}$, $j \in \{1, \dots, M\}$) for all neighborhoods and stores are calculated using the Haversine formula, which measures the shortest arc distance between two sets of latitude and longitude coordinates [Sinnott, 1984]. This formula is implemented in the `distHaversine` function of the `geosphere` package in R [Hijmans, 2022]. It can be used to quickly compute the distances between all neighborhoods and all healthy food stores. For the Piedmont Triad analysis, calculating $387 \times 701 = 271,287$ straight-line distances between $N = 387$ neighborhoods and $M = 701$ stores took 0.1 seconds on a 2020 Macbook Pro (M1 Chip) with 16 gigabytes of memory. Based on straight-line distances D_{ij}^* , the error-prone version of X_i is defined in parallel as $X_i^* = \min(D_{i1}^*, \dots, D_{iM}^*)$.

Select map-based distances D_{ij} ($i \in \{1, \dots, N\}$, $j \in \{1, \dots, M\}$) are calculated using the `mapdist` function from the `ggmap` package in R to query the shortest driving routes between two sets of latitude and longitude coordinates using the Google Maps API [Kahle and Wickham, 2013]. In agreement with the API’s Terms of Service, individual distances D_{ij} were not saved; only the derived variable X_i , computed as the minimum over all j , was saved.

We are interested in the distance to the closest store. However, the closest store by the straight-line distance may not be the closest when using the more accurate map-based distance. Thus, when building the Piedmont Triad data (Section 4), only routes to healthy food stores that were in the lower 20th percentile of straight-line distances for each neighborhood were queried using Google Maps. Across the $N = 387$ neighborhoods, the median distance used as this threshold was 13.4 miles (interquartile range [IQR] = [11, 22.6]). That is, the 20th percentile was chosen as a conservative cutoff; it is unlikely that any healthy food stores farther away could have been the neighborhood’s nearest. Focusing on routes to the $701 \times 0.2 = 140$ nearest stores reduced computation time. Still, calculating $387 \times 701 \times 0.2 = 54,257$ map-based distances took over an hour (4597 seconds) on the same Macbook Pro, compared to the 0.1 seconds to calculate all 271,287 straight-line distances (Supplemental Figure S2).

2.3 Overcoming Missing Map-Based Food Access Data

The error-prone food access variable X^* is observed for all neighborhoods. However, due to computational strain, map-based calculations may only done for a subset of n neighborhoods ($n < N$), leading to missing values of the

error-free food access variable X for the remaining $N - n$ neighborhoods. The missing variable will be multiply imputed for these “unqueried” neighborhoods. The imputed values are introduced first before discussing the multiple imputation framework.

Missing values of map-based proximity, X , will be replaced with random draws from their conditional distributions given their error-prone values, X^* , the log-transformed outcome, $\log(Y)$, and additional fully-observed covariates, \mathbf{Z} . This conditional distribution is assumed to be normal, with mean $= \alpha_0 + \alpha_1 X^* + \alpha_2 \log(Y) + \alpha_3^\top \mathbf{Z}$ and standard deviation $= \sigma$. Estimated parameters for this distribution, denoted by $\hat{\alpha} = (\hat{\alpha}_0, \hat{\alpha}_1, \hat{\alpha}_2, \hat{\alpha}_3, \hat{\sigma})^\top$, are obtained by fitting a linear regression “imputation model” – with X as the outcome and X^* , $\log(Y)$, and \mathbf{Z} as the predictors – to the n “queried” neighborhoods without missing data. Note that the analysis model outcome, $\log(Y)$, must be included in the predictor’s imputation model for the imputation model to be congenial [Moons et al., 2006, D’Agostino McGowan et al., 2024]. Other ways of including the outcome in the imputation model were considered, but using $\log(Y)$ performed best in simulations (Supplemental Figure S3).

These imputed values are incorporated into a multiple imputation framework to obtain valid standard error estimates for statistical inference about the prevalence ratio of interest, $\exp(\beta_1)$. Specifically, the following two-step procedure was adopted from prior work [Shepherd et al., 2012] for each iteration b ($b \in \{1, \dots, B\}$).

1. *Draw imputed values:* Impute missing X with random draws $\check{X}^{(b)}$ from the conditional distribution parameterized by $\hat{\alpha}$. Let $\tilde{X}^{(b)}$ denote the imputed variable from iteration b , where $\tilde{X}^{(b)} = X$ if map-based measures are non-missing and $\tilde{X}^{(b)} = \check{X}^{(b)}$ otherwise.
2. *Fit analysis model to imputed dataset:* Estimate the model of health and food access from Equation (1) with a Poisson regression of Y on $\tilde{X}^{(b)}$ and \mathbf{Z} to obtain parameter and variance estimates, $\hat{\beta}^{(b)}$ and $\hat{V}(\hat{\beta}^{(b)})$, respectively, from iteration b .

For the final analysis, the B sets of estimates are pooled according to Rubin’s rules [Rubin, 2004]. This imputation approach is implemented in the `impPossum` function from the `possum` R package, available on GitHub at <https://github.com/sarahlotspeich/possum>.

3 Simulation Studies

Using data generated to mimic the Piedmont Triad data analyzed in Section 4, we demonstrate how (i) using error-prone, straight-line food access measures can lead to bias, but (ii) incorporating more accurate, map-based food access measures for even a small subset of neighborhoods can correct that bias. Further, imputing map-based food access for neighborhoods where it was missing can offer better efficiency than ignoring those neighborhoods. R scripts to reproduce all simulations, tables, and figures are available on GitHub at https://github.com/sarahlotspeich/food_access_imputation.

3.1 Setup and Data Generation

Samples of $N = 390$ or 2200 neighborhoods were simulated in the following way. (These sample sizes were chosen to represent the Piedmont Triad and the entire state of North Carolina, respectively.) First, map-based proximity to the nearest healthy food store (in miles), X , was generated from a Gamma distribution with shape $= 1$ and scale $= 2.5$. Then, error-prone, straight-line proximity, X^* , was constructed following an additive measurement error model as $X^* = X + U$. The error U was generated from a truncated normal distribution with mean $= \mu_U$, standard deviation $= \sigma_U$, and upper bound $= 0$. (Setting the upper bound to 0 simulates $X^* \leq X$, as expected.) Unless otherwise stated, $\mu_U = -0.7$ and $\sigma_U = 0.8$. Next, the population Pop was generated from a Poisson distribution with mean $= 4165$ people. Finally, the number of cases Y was generated from a Poisson distribution with mean $= Pop \{\exp(-2.7 + 0.01X)\}$, leading to 7% prevalence, on average. A random proportion of $q = 0.1$ neighborhoods were treated as “queried” (i.e., to have non-missing X), while the remaining $1 - q = 0.9$ were treated as “unqueried” (i.e., to have missing X). This proportion relates to the validation study size through $n = \lfloor Nq \rfloor$, where $\lfloor \cdot \rfloor$ denotes the nearest integer function.

The model in Equation (1) was of interest, which captured the association between the neighborhood-level prevalence of the outcome (Y/Pop) and map-based proximity to healthy food stores (X) using Poisson regression. For comparison, this model was fit to the unqueried data (i.e., using X^* for all neighborhoods), the fully queried data (i.e., using X for all neighborhoods), and the partially queried data (i.e., using X and X^* for some neighborhoods and just X^* for the rest). The *gold standard analysis* used the fully queried data to fit the model using Y , Pop , and X from all N

neighborhoods. The *naive analysis* used the unqueried data to fit the model using Y , Pop , and X^* (instead of X) from all N neighborhoods. The *complete-case analysis* used the partially queried data to fit the model using Y , Pop , and X from only the subset of n queried neighborhoods. The *imputation analysis* used the partially queried and unqueried data together to fit the model using Y , Pop , and multiply imputed \tilde{X} (instead of X) from all N neighborhoods $B = 20$ times following the process detailed in Section 2.3.

Empirical relative bias and standard errors for the estimated log prevalence ratio $\hat{\beta}_1$ for map-based proximity X are reported for the four analysis approaches to assess their validity for estimation. For imputation, the average standard error estimates are compared to the empirical standard errors to assess its validity for inference. Among unbiased approaches, relative efficiency to the gold standard analysis is reported to compare statistical precision. Relative efficiency is calculated as the ratio of the empirical variances of the gold standard to the other approaches, with ratios closer to one indicating that more efficiency was recovered.

3.2 Additive Errors in Straight-Line Proximity

Simulation results under increasingly severe additive errors in straight-line proximity to healthy foods X^* are summarized in Table 1. The error magnitude (i.e., severity) was varied by considering different standard deviations $\sigma_U \in \{0.1, 0.2, 0.4, 0.8, 1\}$ for U . For all choices of σ_U , straight-line proximity X^* remained less than or equal to map-based proximity X . With $\hat{\sigma}_U = 0.8$ in the Piedmont Triad data (Section 4.4), more and less severe settings were considered. As expected, the relative bias of the naive analysis grew as σ_U increased and persisted regardless of N . In most cases, the complete-case analysis offered reduced bias over the naive, particularly under more severe errors. Imputation saw lower bias than the naive and complete-case analyses in almost all settings. Even with the smallest sample size and most severe errors, imputation was $< 1\%$ biased.

Table 1: Simulation results under varied additive errors in straight-line proximity to healthy foods, as controlled by the standard deviation σ_U of the errors U .

N	σ_U	Gold Standard		Naive		Complete Case			Imputation				
		Bias	ESE	Bias	ESE	Bias	ESE	RE	Bias	ESE	ASE	CP	RE
390	0.10	0.001	0.001	0.000	0.001	0.003	0.004	0.084	0.002	0.001	0.001	0.946	0.978
	0.20	0.004	0.001	-0.002	0.001	0.005	0.004	0.078	0.004	0.001	0.001	0.958	0.913
	0.40	0.000	0.001	-0.019	0.001	-0.007	0.004	0.080	0.006	0.001	0.001	0.961	0.822
	0.80	0.004	0.001	-0.053	0.001	0.008	0.004	0.093	0.008	0.002	0.002	0.980	0.647
	1.00	-0.005	0.001	-0.082	0.001	-0.010	0.004	0.081	-0.003	0.002	0.002	0.966	0.501
2200	0.10	0.000	0.000	-0.001	0.000	-0.003	0.002	0.087	0.000	0.000	0.001	0.958	0.985
	0.20	0.001	0.001	-0.005	0.001	0.000	0.002	0.106	0.002	0.001	0.001	0.944	0.937
	0.40	-0.001	0.000	-0.021	0.000	0.002	0.002	0.103	0.000	0.001	0.001	0.964	0.840
	0.80	0.000	0.000	-0.054	0.000	0.003	0.002	0.097	0.000	0.001	0.001	0.977	0.601
	1.00	0.000	0.000	-0.077	0.000	0.004	0.002	0.090	0.000	0.001	0.001	0.981	0.547

Note: **Bias** and **ESE** are, respectively, the empirical relative bias and standard error of the log prevalence ratio estimator $\hat{\beta}_1$; **ASE** is the average of the standard error estimator $\widehat{SE}(\hat{\beta}_1)$; **CP** is the empirical coverage probability of the 95% confidence interval for the log prevalence ratio β_1 ; **RE** is the empirical relative efficiency to the Gold Standard. All entries are based on 1000 replicates.

The standard error estimator for imputation performed well, closely approximating the empirical standard error on average. Empirical coverage probabilities for its 95% confidence intervals were close to 0.95. Given the small scale of the true $\beta_1 = 0.01$, the standard errors for all approaches were small. Still, the imputation estimator recovered 50 – 99% of the efficiency of the gold standard analysis, while the complete case analysis only recovered up to 11%. With either N , the imputation estimator recovered more efficiency with smaller σ_U , when the relationship between X and X^* was more informative. Similar observations hold when the error mean μ_U was varied instead (Supplemental Table S1). Thus, imputation performs well under errors in X^* that underestimated X by a bigger margin (driven by larger μ_U) in addition to errors X^* that were noisier about X (due to larger σ_U).

Simulation results with a different proportion $q \in \{0.1, 0.25, 0.5, 0.75\}$ of queried neighborhoods with non-missing X can be found in Table 2. All metrics for the naive analysis, which ignores the queried data, were effectively unchanged across these settings. For any sample size N , the standard errors and, to a lesser extent, the relative bias of the complete-case analysis and imputation estimators decreased as q increased (i.e., when there was less missing data). While the efficiency gains of imputation over the complete-case analysis were largest when q was small, they remained sizeable (relative efficiency 18 – 24% larger) even when q was large.

Table 2: Simulation results with more neighborhoods queried to obtain map-based proximity to healthy foods, as controlled by the proportion $q = n/N$.

N	q	Gold Standard		Naive		Complete Case			Imputation				
		Bias	ESE	Bias	ESE	Bias	ESE	RE	Bias	ESE	ASE	CP	RE
390	0.10	0.004	0.001	-0.053	0.001	0.008	0.004	0.093	0.008	0.002	0.002	0.980	0.647
	0.25	-0.006	0.001	-0.061	0.001	-0.009	0.002	0.230	-0.003	0.001	0.002	0.982	0.789
	0.50	-0.009	0.001	-0.064	0.001	-0.012	0.002	0.472	-0.009	0.001	0.002	0.984	0.913
	0.75	-0.003	0.001	-0.058	0.001	-0.003	0.001	0.730	-0.003	0.001	0.001	0.977	0.973
2200	0.10	0.000	0.000	-0.054	0.000	0.003	0.002	0.097	0.000	0.001	0.001	0.977	0.601
	0.25	0.000	0.000	-0.055	0.000	-0.006	0.001	0.239	0.001	0.001	0.001	0.990	0.841
	0.50	0.002	0.000	-0.053	0.000	0.000	0.001	0.515	0.002	0.001	0.001	0.980	0.919
	0.75	-0.001	0.001	-0.056	0.001	-0.001	0.001	0.785	-0.001	0.001	0.001	0.971	0.968

Note: **Bias** and **ESE** are, respectively, the empirical relative bias and standard error of the log prevalence ratio estimator $\hat{\beta}_1$; **ASE** is the average of the standard error estimator $\widehat{SE}(\hat{\beta}_1)$; **CP** is the empirical coverage probability of the 95% confidence interval for the log prevalence ratio β_1 ; **RE** is the empirical relative efficiency to the Gold Standard. All entries are based on 1000 replicates.

Table 3 summarizes simulations where the disease prevalence and prevalence ratio for map-based food access X were varied. Average disease prevalences (hereafter, simply “prevalences”) of 7%, 11%, and 35% were considered by varying $\beta_0 \in \{\log(0.07), \log(0.11), \log(0.35)\}$, respectively, and prevalence ratios $\exp(\beta_1) \in \{0.95, 0.99, 1, 1.01, 1.05\}$ were included. At the null (i.e., $\beta_1 = 0$), all methods were unbiased, regardless of the prevalence. Beyond that setting, the bias of the naive analysis increased in magnitude as β_1 got farther from zero but was comparable across prevalences. The complete-case and imputation estimators were both virtually unbiased, and the confidence intervals for the imputation estimator achieved proper coverage in all settings. The complete-case analysis only recovered 8 – 9% of the efficiency of the gold standard. Meanwhile, imputation recovered up to 70% at the null but less as β_1 moved away from zero.

Table 3: Simulation results under higher disease prevalence and varied prevalence ratios for map-based proximity to healthy foods, as controlled by the coefficients β_0 (**Prev.** = $\exp(\beta_0)$) and β_1 (**PR** = $\exp(\beta_1)$), respectively.

Prev.	PR	Gold Standard		Naive		Complete Case			Imputation				
		Bias	ESE	Bias	ESE	Bias	ESE	RE	Bias	ESE	ASE	CP	RE
0.07	0.95	0.001	0.001	-0.071	0.002	0.001	0.005	0.092	-0.007	0.003	0.003	0.961	0.279
	0.99	-0.006	0.001	-0.066	0.001	-0.040	0.004	0.087	-0.004	0.002	0.002	0.967	0.589
	1.00	0.000	0.001	0.000	0.001	0.000	0.004	0.079	0.000	0.002	0.002	0.973	0.618
	1.01	0.011	0.001	-0.046	0.001	0.025	0.004	0.081	0.016	0.002	0.002	0.965	0.593
	1.05	0.000	0.001	-0.046	0.001	0.001	0.004	0.078	0.014	0.002	0.003	0.966	0.205
0.11	0.95	0.000	0.001	-0.072	0.001	0.001	0.004	0.091	-0.008	0.002	0.003	0.960	0.225
	0.99	0.003	0.001	-0.059	0.001	0.002	0.003	0.086	-0.002	0.001	0.001	0.969	0.585
	1.00	0.000	0.001	0.000	0.001	0.000	0.003	0.080	0.000	0.001	0.001	0.975	0.640
	1.01	0.002	0.001	-0.054	0.001	0.000	0.003	0.086	0.006	0.001	0.001	0.962	0.532
	1.05	0.000	0.001	-0.046	0.001	-0.003	0.003	0.082	0.010	0.002	0.002	0.970	0.158
0.33	0.95	0.000	0.001	-0.072	0.001	0.001	0.002	0.085	-0.012	0.002	0.002	0.954	0.134
	0.99	-0.001	0.001	-0.061	0.001	0.003	0.002	0.089	-0.005	0.001	0.001	0.962	0.482
	1.00	0.000	0.001	0.000	0.001	0.000	0.002	0.075	0.000	0.001	0.001	0.986	0.703
	1.01	0.003	0.001	-0.052	0.001	0.008	0.002	0.085	0.002	0.001	0.001	0.966	0.449
	1.05	0.000	0.000	-0.046	0.001	0.002	0.002	0.080	0.004	0.002	0.002	0.968	0.084

Note: **Bias** and **ESE** are, respectively, the empirical relative bias and standard error of the log prevalence ratio estimator $\hat{\beta}_1$; **ASE** is the average of the standard error estimator $\widehat{SE}(\hat{\beta}_1)$; **CP** is the empirical coverage probability of the 95% confidence interval for the log prevalence ratio β_1 ; **RE** is the empirical relative efficiency to the Gold Standard. All entries are based on 1000 replicates.

3.3 Multiplicative Errors in Straight-Line Proximity

Error-prone X^* was also simulated from a multiplicative error model such that $X^* = WX$. Random errors W were generated from a truncated Normal distribution with mean = 0.7, standard deviation = σ_W , and upper bound = 1. (Setting the maximum to 1 simulated straight-line proximity to be strictly less than or equal to map-based, as expected.) Different standard deviations $\sigma_W \in \{0.1, 0.15, 0.2\}$ were considered for W , where smaller values led to less severe

errors in X^* . With $\hat{\sigma}_W = 0.15$ in the Piedmont Triad data, more and less severe settings were considered. All other variables were simulated following Section 3.1.

Simulation results under increasingly severe multiplicative errors in straight-line proximity to healthy foods are described in Table 4. The naive analysis was considerably more biased in the multiplicative error settings considered than under the additive ones in Section 3.2 (as high as 37% versus 8%). The complete-case analysis offered low bias ($\leq 1\%$) but low efficiency (10% or less recovered) in all settings. The imputation estimator offered similarly low bias ($< 2\%$) with much higher efficiency (39 – 62% recovered). Its standard error estimator and confidence intervals remained valid in all settings. As with additive errors, the imputation estimator recovered more efficiency in the least severe settings (i.e., with smaller σ_W) in small or large samples.

Table 4: Simulation results under varied multiplicative errors in straight-line proximity to healthy foods, as controlled by the standard deviation σ_W of the errors W .

N	σ_W	Gold Standard		Naive		Complete Case			Imputation				
		Bias	ESE	Bias	ESE	Bias	ESE	RE	Bias	ESE	ASE	CP	RE
390	0.10	-0.002	0.001	0.373	0.002	-0.004	0.004	0.082	-0.011	0.002	0.002	0.940	0.618
	0.15	0.001	0.001	0.335	0.002	-0.006	0.004	0.085	-0.010	0.002	0.002	0.949	0.510
	0.20	-0.008	0.001	0.298	0.002	-0.007	0.004	0.084	-0.015	0.002	0.002	0.959	0.426
2200	0.10	-0.003	0.000	0.370	0.001	-0.004	0.002	0.094	-0.006	0.001	0.001	0.959	0.618
	0.15	0.001	0.000	0.335	0.001	0.011	0.002	0.100	-0.008	0.001	0.001	0.956	0.455
	0.20	0.002	0.000	0.309	0.001	-0.005	0.002	0.099	-0.007	0.001	0.001	0.965	0.391

Note: **Bias** and **ESE** are, respectively, the empirical relative bias and standard error of the log prevalence ratio estimator $\hat{\beta}_1$; **ASE** is the average of the standard error estimator $\widehat{\text{SE}}(\hat{\beta}_1)$; **CP** is the empirical coverage probability of the 95% confidence interval for the log prevalence ratio β_1 ; **RE** is the empirical relative efficiency to the Gold Standard. All entries are based on 1000 replicates.

4 Application to the Piedmont Triad, North Carolina

The Piedmont Triad, located in the northwestern region of North Carolina, comprises twelve counties. Beyond two medium-sized cities (Greensboro and Winston–Salem), much of the area is rural, with a median population density for neighborhoods (census tracts) across the region of 843 people per square mile (minimum = 33, maximum = 6681). The region includes one neighborhood with zero population, which contains only the Piedmont Triad International Airport and is excluded from all analyses. The $N = 387$ neighborhoods in the Piedmont Triad are described in Supplemental Table S2. The number of neighborhoods per county varied from as few as six in the rural counties to as many as 118 in the urban ones. According to the 2010 U.S. Census, the median population per neighborhood was 4095 people (IQR = [3901, 5282]). Land area per census tract was 5 square miles, on average (IQR = [2, 19]).

The socioeconomic factors vary substantially between neighborhoods in this region. A brief socioeconomic profile, based on the 2015 American Community Survey (ACS), is illustrated in Supplemental Figure S4. The median household income was \$53,750, on average, but was as low as \$13,447 and as high as \$176,875. The percentage of neighborhood households with income below the poverty line varies widely and ranges from 0% and 73%. Most neighborhoods had low proportions of households receiving the Supplemental Nutrition Assistance Program (SNAP) (median = 13%). Still, there were some neighborhoods with as many as 75% who were receiving this type of government assistance. Most workers ($\geq 45\%$) in nearly all neighborhoods drive alone to work; still, a neighborhood where 97% of workers drive alone (the maximum) would be very different than one where 45% do (the minimum). The proportion of people with health insurance (public or private) varied some (between 65% and 100%), although not as much as other variables like the proportion of people 25 years or older who completed at least some college (between 26% and 96%) and the others mentioned thus far.

4.1 Motivation for Analysis

Preliminary data using straight-line proximity to healthy foods suggest that many neighborhoods in the Piedmont Triad, NC, have few options close to home (Figure 1). The actual number of neighborhoods with poor access to healthy foods is likely even higher, since map-based proximity has to be as bad as or worse than straight-line proximity. This concern is echoed by data reported from the Economic Research Service (ERS), U.S. Department of Agriculture (USDA) [2019], wherein 46% and 67% of neighborhoods in the Piedmont Triad were found to have high proportions of people living more than 1 mile and 0.5 mile, respectively, from their nearest supermarket. Many neighborhoods without

access are in Forsyth and Guilford County, putting these counties among the least accessible in the state. Interestingly, Forsyth and Guilford are both relatively urban counties, whereas one might expect lower access in more expansive, rural areas. However, beyond these cities' largest cities (Winston-Salem and Greensboro, respectively), there are many rural neighborhoods that could help explain this result.

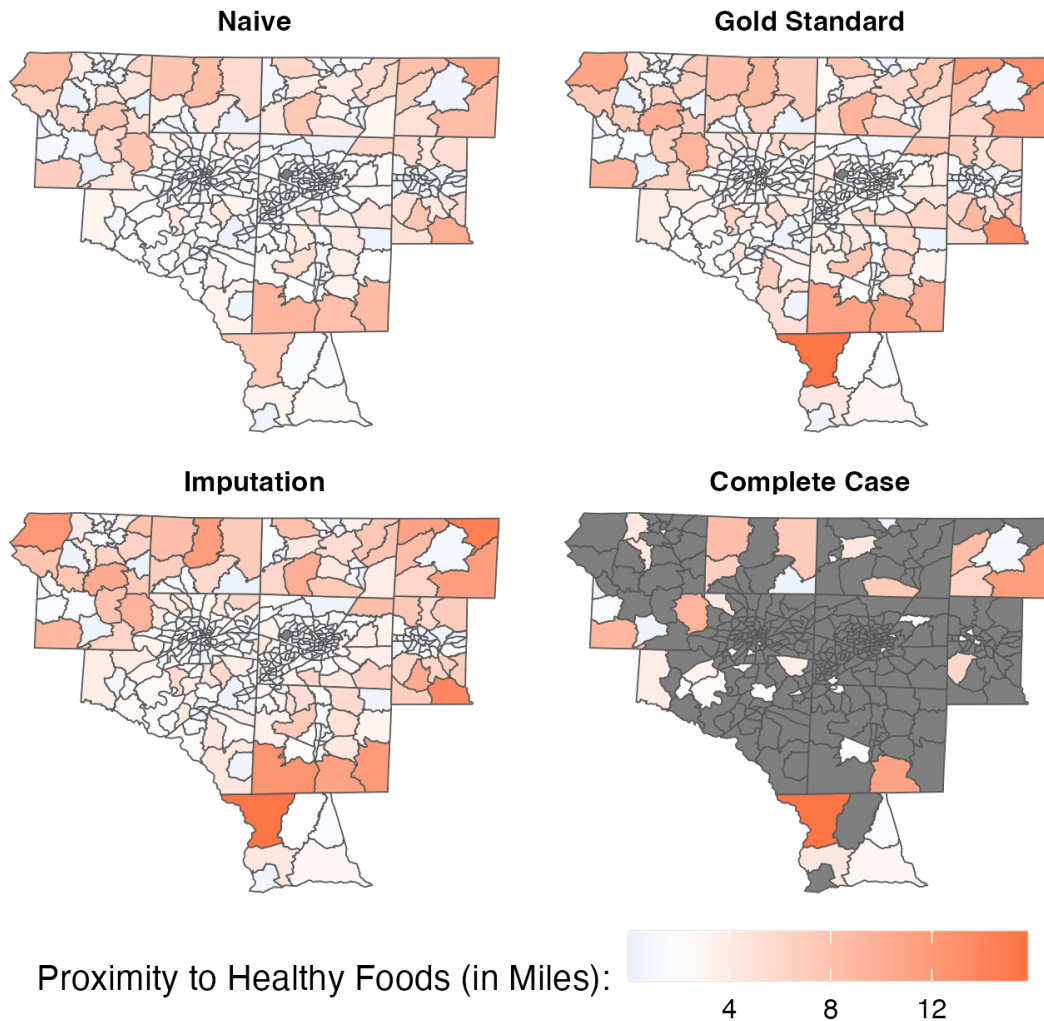


Figure 1: Choropleth map of food access, as measured by proximity to healthy foods for each neighborhood (census tract) in the Piedmont Triad, North Carolina, according to the data used for the naive, gold standard, imputation, and complete-case analyses.

National studies in the U.S. have previously found links between diabetes and obesity and the availability of healthy foods. Ahern et al. [2011] found that lower county-level prevalence of type 2 diabetes was associated with having more “healthy” food options (full-service restaurants, grocery stores, direct farm sales). Kanchi et al. [2021] found that higher relative densities of supermarkets to other retail food outlets were associated with lessened risk of incident type 2 diabetes in a national cohort study of U.S. veterans. Ahern et al. [2011] also found full-service restaurants and direct farm sales to be associated with lower county-level prevalence of obesity, while grocery stores were associated with

higher rates. However, other studies have found conflicting evidence on these connections between food access and health [e.g., White, 2007], so it is critical to re-investigate these relationships for the Piedmont Triad alone.

4.2 Data Collection

Publicly available data were combined from three sources for the analysis using open-source tools in R [R Core Team, 2023]. The *tidycensus* package was used to extract ACS data and create maps [Walker and Herman, 2024]. Links to the datasets and all R code are available on GitHub at https://github.com/sarahlotspeich/food_access_imputation.

Diabetes and obesity prevalence estimates were taken from the U.S. Centers for Disease Control and Prevention’s 2022 PLACES dataset [Centers for Disease Control and Prevention, 2022]. Like other administrative datasets, PLACES contains small area estimates (SAEs) of prevalence, which were obtained via statistical modeling using individual- and area-level information (e.g., age, education, poverty) as predictors [Centers for Disease Control and Prevention, 2023]. The PLACES data were available at the census tract level, which was adopted as the “neighborhood” unit for analysis.

Store locations and types were obtained from the U.S. Department of Agriculture’s 2022 Historical SNAP Retail Locator Data [United States Department of Agriculture, 2022] to calculate neighborhoods’ proximity to healthy foods. The analysis used $M = 701$ NC farmers’ markets, grocery stores (any size), specialties (baker, fruits/vegetables, meat/poultry, seafood), and supermarkets/stores as “healthy food stores.” A map of stores by type can be found in Supplemental Figure S5.

With a moderate number of neighborhoods in the Piedmont Triad ($N = 387$ census tracts), we were actually able to establish the gold standard here, which would not always be possible in practice. Using Google Maps and the Haversine formula for distance calculations, we collected map-based and straight-line proximity, respectively, to healthy foods for the entire region. Then, map-based proximity X from these fully queried data was used to fit the gold standard analysis. The naive analysis used straight-line proximity X^* from the unqueried data instead.

For the complete-case and imputation analyses, an artificial partially queried dataset was also constructed, wherein only $n = 48$ census tracts ($q = 0.12$) had map-based X available. To ensure geographic diversity of this queried subset, four neighborhoods were chosen from each county to be treated as queried and have map-based proximity X available (Supplemental Figure S6). Many other sampling designs are possible, and targeted strategies are a promising direction for future work.

4.3 Health in the Piedmont Triad

There is between-neighborhood variability in the prevalences of diagnosed diabetes and obesity outcomes seen across the Piedmont Triad (Figure 2). Contrasts are seen between (i) rural and urban neighborhoods but also (ii) neighborhoods surrounding the same major city. Overall, the regional average prevalences for obesity (median = 0.34, IQR = [0.31, 0.38]) and diabetes (median = 0.11, IQR = [0.09, 0.13]) were comparable to the state averages (0.1 and 0.34, respectively). Most larger, rural neighborhoods had prevalences of diabetes and obesity that were above the state averages. In contrast, many smaller urban neighborhoods saw lower burdens of these diseases. When zooming in on Forsyth or Guilford County, there seem to exist divisions between neighborhoods with low and high prevalences on opposite sides of their major cities’ downtown areas (Supplemental Figure S7). Socioeconomic differences could potentially drive these divisions, further highlighting the complexity in accounting for the complete picture when analyzing social determinants of health.

4.4 Proximity to Healthy Foods in the Piedmont Triad

From the fully queried data ($N = 387$ neighborhoods), the following could be learned about straight-line and map-based food access, as well as their relationship. Across all neighborhoods in the Piedmont Triad, proximity to healthy foods based on map-based distances was farther, on average, than the same measure based on straight-line distances, as expected (median proximity = 1.01 versus 1.51 miles). The variability of map-based proximity was larger than that of straight-line proximity, also (IQR = [0.89, 2.99] versus [0.57, 2.12]). Still, the two proximity measures were very highly correlated ($R = 0.97$), and the relationship between them was linear (Figure 3).

When comparing food access between neighborhoods, the straight-line and map-based measures depicted similar trends across the Piedmont Triad, with better proximity (shorter distances) around urban areas and worse proximity (larger distances) in the rural surrounds (Figure 1). Some rural tracts with poor straight-line proximity had even worse access to healthy foods according to the map-based measure. For example, the nearest healthy food retailer to the population center of Census Tract 9301 within Caswell County was 10.8 miles away according to the straight-line distances (the

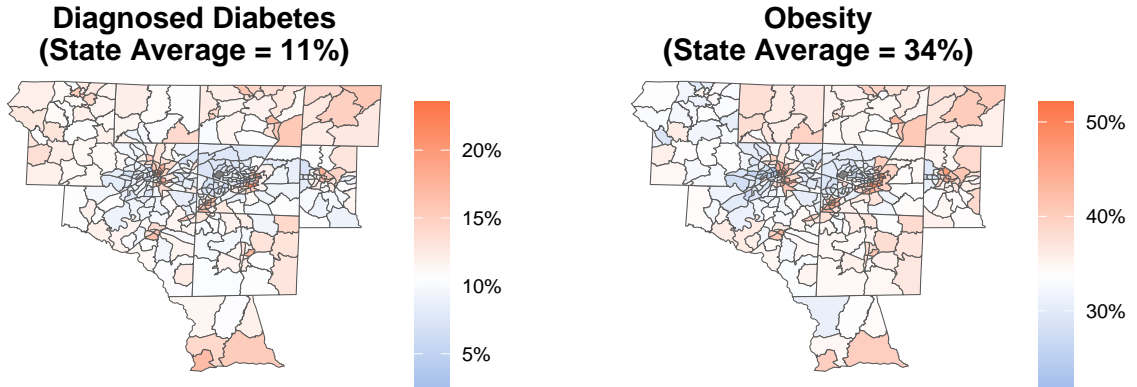


Figure 2: Choropleth maps of the crude prevalence of diagnosed diabetes and obesity for census tracts in the Piedmont Triad, North Carolina. The gradient for each map is centered at the state median. Data were taken from the 2022 PLACES dataset [Centers for Disease Control and Prevention, 2022]. One census tract was excluded because it had a population of zero.

worst in the Piedmont Triad). Using map-based distances instead, proximity to healthy foods in this tract was 13.1 miles (the third-worst instead). There were also instances where straight-line proximity was pretty poor, but map-based proximity uncovered noticeably worse access to healthy foods. For example, Census Tract 9603 within Montgomery County had straight-line proximity of 7.3 miles (among the 15 worst in the Piedmont Triad) but map-based proximity of 15.8 miles (the worst in the area).

The magnitude of the errors in straight-line proximity was also calculated using the fully queried data. First, an additive error mechanism was considered. On average, straight-line proximity X^* underestimated map-based proximity X by 0.7 miles (i.e., $\hat{\mu}_U = -0.7$). Most neighborhoods (77%) had straight-line proximity X^* that underestimated their map-based proximity X by no more than one mile. However, the distribution of additive errors across the Piedmont Triad was left-skewed (Supplemental Figure S8), with the largest additive error of $U = -8.42$. This skewness can also be seen when comparing the mean and median magnitude of the errors, -0.7 and -0.5 , respectively, as the former is influenced more by the larger errors in the tail of the distribution. The standard deviation of the additive errors $\hat{\sigma}_U = 0.8$ was one of the most severe settings considered in the simulations (Section 3.2).

Next, a multiplicative error mechanism was considered. On average, straight-line proximity underestimated map-based proximity by 30% (i.e., $\hat{\mu}_W = 0.70$). The distribution of the multiplicative errors was much more symmetric (Supplemental Figure S8). There were still some neighborhoods with much more extreme errors than others; interestingly, they were different from the neighborhoods with the worst additive ones. The most severe multiplicative error ($W = 0.063$) was seen for Census Tract 315.04 within Randolph County, among the neighborhoods with additive errors under one mile in magnitude ($U = -0.92$). The standard deviation of the multiplicative errors $\hat{\sigma}_W = 0.15$ was chosen as the moderate setting for simulations (Section 3.3).

4.5 Imputation Models for Straight-Line Proximity

For each health outcome, the imputation of map-based proximity to healthy foods X began by fitting the imputation model described in Section 2.3. For diagnosed diabetes, $\hat{\mu} = 1.227 + 1.369X^* - 0.196 \log(Y)$ and $\hat{\sigma} = 1.057$. For obesity, $\hat{\mu} = 3.330 + 1.372X^* - 0.318 \log(Y)$ and $\hat{\sigma} = 1.053$. For simplicity and given the high $R^2 \approx 0.91$, additional covariates \mathbf{Z} (e.g., a rural/urban indicator) were not included in the imputation models, but doing so would be straightforward.

Using these estimates, each census tract missing X in the partially queried dataset was multiply imputed $B = 20$ times for the imputation analyses. Imputing the missing X values for the unqueried neighborhoods allowed them to contribute to the disease models in Section 4.6. The imputed X values can also be used to supplement the subset of queried data and create a more accurate and complete description of the landscape of food access in the Piedmont Triad than the

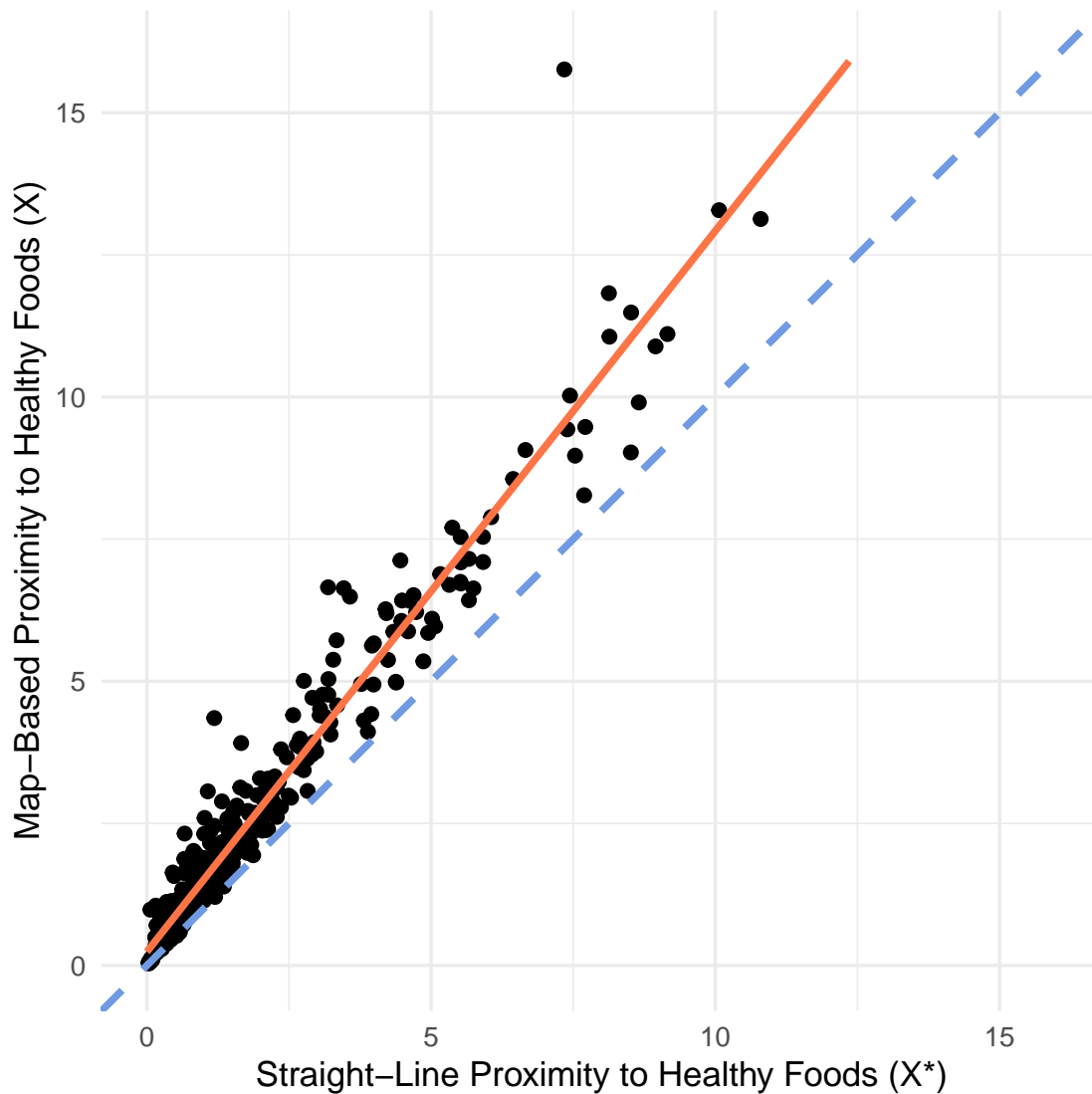


Figure 3: Scatter plot of straight-line versus map-based proximity to healthy food store for neighborhoods (census tracts) in the Piedmont Triad, North Carolina using the fully queried data ($N = 387$). The solid line follows the fitted least-squares linear regression fit between X and X^* , while the dashed line denotes the hypothetical $X = X^*$ if there had been no errors in X^* .

naive and complete case analyses, respectively. In Figure 1, the map of proximity to healthy foods based on a single imputation (not including $\log(Y)$) is (i) far more comprehensive than the one based on the complete case (ignoring data for 339 of 387 census tracts) and (ii) more similar to the gold standard than the one based on the naive.

4.6 Modeling the Connection Between Proximity and Disease

Finally, the connections between proximity to healthy foods and the prevalence of each health outcome across neighborhoods (census tracts) in the Piedmont Triad were modeled using Poisson regression. In contrast to the simulations, neighborhoods closer together in space could be more similar than to neighborhoods farther away. To

evaluate this potential spatial correlation, Moran’s I was calculated for both diseases of interest using the *spdep* package in R [Pebesma and Bivand, 2023]. Specifically, Moran’s I was calculated for the residuals $e_i^* = Y_i - \hat{Y}_i^*$ from the naive analysis, where Y_i and $\hat{Y}_i^* = \exp(\hat{\beta}_0^* + \hat{\beta}_1^* X_i) Pop_i$ denote the observed and predicted number of cases in neighborhood i , respectively. The parameters $(\hat{\beta}_0^*, \hat{\beta}_1^*)$ were taken from the naive models, which would have fully available data in practice and should be highly correlated with the gold standard ones. Both diagnosed diabetes ($I = 0.057, p = 0.023$) and obesity ($I = 0.059, p = 0.018$) had spatial autocorrelation that would be considered statistically significant at the $\alpha = 0.05$ significance level.

A conditional autoregressive (CAR) model was used to capture the connections between proximity to healthy foods and health outcomes while allowing for spatial autocorrelation between neighborhoods that share a border. This model can be defined as a mixed-effects Poisson regression with a random intercept for each neighborhood based on its bordering neighborhoods. Thus, instead of Equation (1),

$$\log\{E_{\beta}(Y|X)\} = \beta_0 + \beta_1 X + r + \log(Pop), \quad (2)$$

was of interest in the Piedmont Triad data, where r denotes a neighborhood-specific random intercept. The vector of all neighborhoods’ random intercepts $\mathbf{r} = (r_1, \dots, r_N)^\top$ is assumed to follow a multivariate normal distribution with mean vector $\mathbf{0}$ and covariance matrix Σ defined to allow bordering neighborhoods to be correlated. See Waller and Gotway [2004] for more technical details on the CAR model. While the random intercepts \mathbf{r} may be correlated with each other, they are independent of the access variables $\mathbf{X} = (X_1, \dots, X_N)^\top$. Using the `fitme` function from the *spaMM* package in R [Rousset and Ferdy, 2014], Equation (2) was estimated following the gold standard, naive, complete case, and imputation analysis approaches. For reference, the non-spatial models, estimating Equation (1), were also fit. Additional covariates \mathbf{Z} were not included since many of the individual- and area-level factors that might be controlled for here could have already been used in the small area estimation of Y [Centers for Disease Control and Prevention, 2023].

4.7 Findings from the Piedmont Triad

The prevalence ratio between two census tracts whose proximities to healthy foods differed by 1 mile ($PR = \exp(\beta_1)$) was of primary interest. Forest plots of the estimated prevalence ratios ($\widehat{PR} = \exp(\hat{\beta}_1)$) from each analysis method, along with their 95% confidence intervals (95% CI), are included in Figure 4. Based on the gold standard analysis, worse access to healthy foods (i.e., larger distances X to the nearest healthy foods retailer) was associated with slightly *lower* prevalence of obesity ($\widehat{PR} = 0.994$, 95% CI: 0.989, 1.000). That is, for every 1 mile farther a census tract’s nearest healthy foods retailer is from its population center, its prevalence of obesity is expected to decrease by 0.6%. This result aligns with the previous findings of Kanchi et al. [2021]. However, the confidence interval did touch the null ($PR = 1$). For diagnosed diabetes, the estimated prevalence ratio was close to the null ($\widehat{PR} = 0.997$), and the confidence interval contained one (95% CI: 0.987, 1.008).

For diagnosed diabetes, the naive estimate was biased toward the null, while for obesity, the naive estimate closely resembled the gold standard. The confidence intervals were slightly wider, leading the 95% CI for obesity to cross the null ($\widehat{PR} = 0.994$, 95% CI: 0.987, 1.001). Still, the naive analysis led to the same conclusion about the absence of an association between proximity and diagnosed diabetes ($\widehat{PR} = 0.999$, 95% CI: 0.985, 1.014).

The estimated prevalence ratio for diagnosed diabetes ($\widehat{PR} = 0.986$) from the complete case analysis was farther from the null than that for the gold standard analysis. Still, its wider confidence interval (95% CI: 0.9721, 1.002) captured the null. Notably, the complete case analysis should be asymptotically consistent since X is missing at random (MAR) [Little, 1992] for the unqueried neighborhoods, but there are no such guarantees in a small sample like this one ($n = 48$). These differences could also be explained by the higher estimated baseline prevalence, i.e., the predicted disease prevalence in a census tract where proximity to healthy foods was 0 miles (Supplemental Figure S9). The complete-case estimate for obesity ($\widehat{PR} = 0.993$, 95% CI: 0.984, 1.002) was in line with the gold standard and naive. Thus, based on the complete case analysis, the conclusion would be that neither health outcome was significantly associated with proximity to healthy foods.

As expected, the imputation analysis fell in many ways between the naive, gold standard, and complete case analyses. The imputation prevalence ratio estimates for both outcomes closely resembled those from the gold standard analysis. They were notably closer for diagnosed diabetes ($\widehat{PR} = 0.998$, 95% CI: 0.984, 1.013) than the complete case analysis estimates. The four analysis methods were very similar for obesity ($\widehat{PR} = 0.996$, 95% CI: 0.986, 1.005). As with the complete case, the wider confidence intervals from the imputation analysis both captured the null. Therefore, neither health outcome would be considered significantly associated with neighborhood proximity to healthy foods. Imputation’s efficiency gain over the complete case analysis was not seen in the Piedmont Triad data like in the

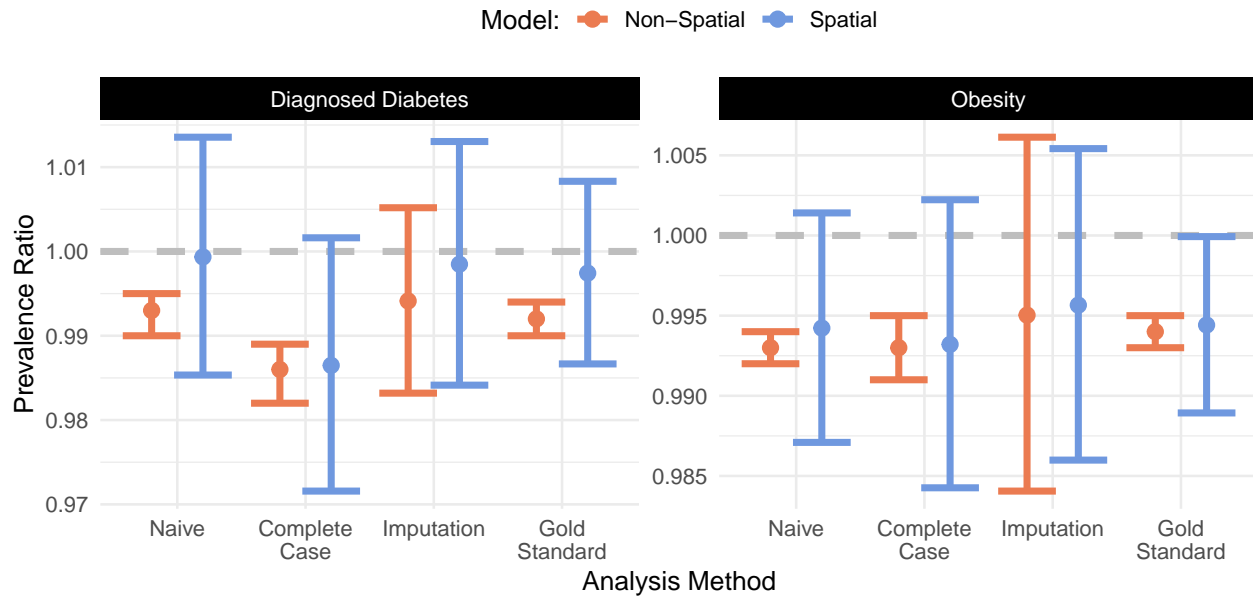


Figure 4: Estimated prevalence ratios (with 95% confidence intervals) for proximity to healthy foods and health outcomes in the Piedmont Triad, North Carolina using different analysis methods. Within each health outcome and method, estimates on the right came from the mixed effects model allowing for spatial autocorrelation between neighboring census tracts; estimates on the left came from the model assuming independence between tracts.

simulations (Section 3). As discussed in Section 4.4, the errors in these data aligned with the moderate-to-severe simulation settings considered, which could explain some of the efficiency loss.

The most notable difference for the non-spatial models was the smaller standard errors relative to the spatial models for either outcome and almost all analysis methods. Importantly, different conclusions would have been drawn from the non-spatial models, as the smaller standard errors led to narrower 95% CIs. In the gold standard analysis, both health outcomes could be considered significantly associated with proximity to healthy foods. Specifically, farther proximity (worse access) would be significantly associated with lower prevalences of diagnosed diabetes and obesity. These differences in conclusions demonstrate the importance of modeling spatial data accordingly, as ignoring the autocorrelation between neighboring census tracts could lead to incorrect conclusions about the relationships of interest. There could also be unmeasured confounding (e.g., due to socioeconomic differences), since these models did not adjust for additional covariates.

5 Conclusion

Eating healthy food is a critical determinant of healthy living, yet many communities have inadequate access to fresh, nutritious food. Given the public health ramifications of disparities in food access and their potential connection to disparities in health, accurately identifying low-access, high-risk communities is a priority. Quantifying access requires an extensive number of distance calculations (e.g., between neighborhood population centers and healthy food stores), and these calculations are either (i) computationally simple methods but inaccurate or (ii) accurate methods but computationally complex. This trade-off is solved by adopting a partial validation study design and then devising a multiple imputation for measurement error framework to overcome the missing data. In doing so, our approach offers improved accuracy in quantifying food access and modeling its impact on health with computational ease. The proposed methods make large-scale analyses of accurate distance-based access measures feasible by overcoming the computational hurdles. Therefore, the geographic scope of access studies can expand to answer questions and drive decision-making for larger communities.

Imputation was preferable over other model-based methods here for a few reasons. First, the covariate imputation framework can be used with various outcome models, whereas maximum likelihood estimators [e.g., Tang et al., 2015] need to be re-derived for any model changes. This flexibility was demonstrated in the real data analysis, where spatial correlation between disease prevalences in bordering neighborhoods was detected and incorporated into the analysis model with ease. Second, under correct analysis and imputation model specification, imputation offers consistent

estimates in Poisson regression. Regression calibration is only approximately unbiased for nonlinear outcome models, although it has been found to work fairly well Shaw et al. [2020].

In simulations, imputation captures the benefits of the more accurate, map-based access data despite this data being largely missing. Notably, the simulations also demonstrate that the proposed methods offered unbiased, often highly efficient estimates under either additive or multiplicative error mechanisms, making the methods broadly applicable to other modeling approaches for access and health. With the naive analysis shown to be biased toward or away from the null, the importance of accurately measuring access was illustrated in simulations and the Piedmont Triad analysis.

The Poisson regression model makes the assumption of equal dispersion (i.e., equal mean and variance) for the analysis model, which may not be reasonable in practice. Fortunately, it would be straightforward to adapt the multiple imputation procedure here to another model, like negative binomial regression, if over- or underdispersion were present. In the real data, imputation's efficiency gains over the complete case analysis were not as clear as in the simulations, but its estimates remained closer to the gold standard. Another limitation related to the Piedmont Triad analysis is using disease counts Y that are predictions from their own models. Therefore, though many of these socioeconomic variables may have been relevant to the analysis models here, additional covariates Z were not included since they were potentially already used to predict Y . Defining the origin for distance calculations from the census tracts posed one final challenge. A central point was used to measure access for all residents, smoothing over the gradient of access within a census tract.

There are several interesting directions for future work. First, the subset of queried neighborhoods can be sampled based on any fully available information, providing an opportunity for strategic design. Perhaps existing optimal designs for Poisson regression [e.g., Wang et al., 2006] or measurement error in other models [e.g., Amorim et al., 2021, Lotspeich et al., 2024] could be adapted. Second, map-based driving distance was used to gauge neighborhood proximity. With map-based driving time as another metric of food access that is expensive to obtain, it could be interesting to impute time-based food access from straight-line measures instead. Third, neighborhood rates of disease could also be related to *unhealthy* foods access, or whichever type of food (healthy or unhealthy) is more accessible.

References

- S. Liu, J. E. Manson, I. M. Lee, S. R. Cole, C. H. Hennekens, W. C. Willett, and J. E. Buring. Fruit and vegetable intake and risk of cardiovascular disease: the Women's Health Study. *The American Journal of Clinical Nutrition*, 72(4): 922–928, 2000.
- A. H. Harding, N. J. Wareham, S. A. Bingham, K. Khaw, A. Luben, R. Welch, and N. G. Forouhi. Plasma vitamin C level, fruit and vegetable consumption, and the risk of new-onset type 2 diabetes mellitus: the European Prospective Investigation of Cancer–Norfolk Prospective Study. *Archives of Internal Medicine*, 168(14):1493–1499, 2008.
- K. M. Bower, R. J. Thorpe, C. Rohde, and D. J. Gaskin. The intersection of neighborhood racial segregation, poverty, and urbanicity and its impact on food store availability in the United States. *Journal of Disability Policy Studies*, 58: 33–39, 2014.
- D. L. Brucker and A. Coleman-Jensen. Food insecurity across the adult lifespan for persons with disabilities. *Journal of Disability Policy Studies*, 28(2):109–118, 2017.
- N. Bennion, A.H. Redelfs, L. Spruance, S. Benally, and C. Sloan-Aagard. Driving distance and food accessibility: a geospatial analysis of the food environment in the Navajo nation and border towns. *Frontiers in Nutrition*, 9:904119, 2022.
- M.P. Burke, S. J. Jones, E. A. Frongillo, M. S. Fram, C. E. Blake, and D. A. Freedman. Severity of household food insecurity and lifetime racial discrimination among African-American households in South Carolina. *Ethnicity & Health*, 23(3):276–292, 2018.
- A. Odoms-Young and M. A. Bruce. Examining the impact of structural racism on food insecurity: Implications for addressing racial/ethnic disparities. *Family & Community Health*, 41:S3–S6, 2018.
- M. Ahern, C. Brown, and S. Dukas. A national study of the association between food environments and county-level health outcomes. *The Journal of Rural Health*, 27:367–379, 2011.
- D. Gallegos, A. Eivers, P. Sondergeld, and C. Pattinson. Food insecurity and child development: A state-of-the-art review. *International Journal of Environmental Research and Public Health*, 18(17):8990, 2021.
- R. Kanchi, P. Lopez, P. E. Rummo, D. C. Lee, S. Adhikari, M. D. Schwartz, S. Avramovic, K. R. Siegel, D. B. Rolka, G. Imperatore, B. Elbel, and L. E. Thorpe. Longitudinal analysis of neighborhood food environment and diabetes risk in the Veterans Administration Diabetes Risk Cohort. *JAMA Network Open*, 4(10):e2130789, 2021.

- Y. Li, S. Wang, G. Cao, D. Li, and B. P. Ng. Disentangling racial/ethnic and income disparities of food retail environments: Impacts on adult obesity prevalence. *Applied Geography*, 137:102607, 2021.
- N. I. Larson, M. T. Story, and M. C. Nelson. Neighborhood environments: disparities in access to healthy foods in the U.S. *American Journal of Preventive Medicine*, 36(1):74–81, 2009.
- E. Titis, R. Procter, and L. Walasek. Assessing physical access to healthy food across United Kingdom: A systematic review of measures and findings. *Obesity Science & Practice*, 8(2):233–246, 2021.
- K. Peng, D. A. Rodríguez, M. Peterson, L. M. Braun, A. G. Howard, C. E. Lewis, J. M. Shikany, and P. Gordon-Larsen. GIS-based home neighborhood food outlet counts, street connectivity, and frequency of use of neighborhood restaurants and food stores. *Journal of Urban Health*, 97(2):213–225, 2020.
- B. N. Sánchez, M. Fu, H. Matsuzaki, and E. Sanchez-Vaznaugh. Characterizing food environments near schools in California: A latent class approach simultaneously using multiple food outlet types and two spatial scales. *Preventive Medicine Reports*, 29:101937, 2022.
- J. R. Sharkey, S. Horel, D. Han, and Jr Huber, J. C. Association between neighborhood need and spatial access to food stores and fast food restaurants in neighborhoods of colonias. *International Journal of Health Geographics*, 8:9, 2009.
- M. Matsuzaki, E. V. Sanchez-Vaznaugh, K. Alexovitz, M. E. Acosta, and B. N. Sánchez. Trends in school-neighbourhood inequalities and youth obesity: Repeated cross-sectional analyses of the public schools in the state of California. *Pediatric Obesity*, 18(3):e12991, 2023.
- R Core Team. *R: A Language and Environment for Statistical Computing*. R Foundation for Statistical Computing, Vienna, Austria, 2023. URL <https://www.R-project.org/>.
- David Kahle and Hadley Wickham. ggmap: Spatial visualization with ggplot2. *The R Journal*, 5(1):144–161, 2013. URL <https://journal.r-project.org/archive/2013-1/kahle-wickham.pdf>.
- David Cooley. *googleway: Accesses Google Maps APIs to Retrieve Data and Plot Maps*, 2023. URL <https://CRAN.R-project.org/package=googleway>. R package version 2.7.7.
- R. J. Carroll, D. Ruppert, L. A. Stefanski, and C. M. Crainiceanu. *Measurement Error in Nonlinear Models: a Modern Perspective*. Boca Raton: Chapman and Hall/CRC, 2006.
- J.E. White. A two stage design for the study of the relationship between a rare exposure and a rare disease. *American Journal of Epidemiology*, 115(1):119–128, 1982.
- M. J. Giganti, P. A. Shaw, G. Chen, S. S. Bebawy, M. M. Turner, T. R. Sterling, and B. E. Shepherd. Accounting for dependent errors in predictors and time-to-event outcomes using electronic health records, validation samples, and multiple imputation. *The Annals of Applied Statistics*, 14(2):1045–1061, 2020.
- L. Nab, M. van Smeden, R. de Mutsert, F. R. Rosendaal, and R. H. H. Groenwold. Sampling strategies for internal validation samples for exposure measurement-error correction: A study of visceral adipose tissue measures replaced by waist circumference measures. *American Journal of Epidemiology*, 190(9):1935–1947, 2021.
- S.C. Lotspeich, B.E. Shepherd, G.G.C. Amorim, P.A. Shaw, and R. Tao. Efficient odds ratio estimation under two-phase sampling using error-prone data from a multi-national HIV research cohort. *Biometrics*, 78(4):1674–1685, 2022.
- W. Fuller. *Measurement Error Models*. New York: Wiley, 1987.
- B. A. Barron. The effects of misclassification on the estimation of relative risk. *Biometrics*, 33(2):414–418, 1977.
- J. V. Videk and H. Wong. Causality, measurement error, and multicollinearity in epidemiology. *Environmetrics*, 7: 441–451, 1996.
- D. G. Horvitz and J. D. Thompson. A generalization of sampling without replacement from a finite universe. *Journal of the American Statistical Association*, 47(260):663–685, 1952.
- J. C. Deville, C. E. Sarndal, and O. Sautory. Generalized raking procedures in survey sampling. *Journal of the American Statistical Association*, 88(423):1013–1020, 1993.
- J. M. Robins, A. Rotnitzky, and L. P. Zhao. Estimation of regression coefficients when some regressors are not always observed. *Journal of the American Statistical Association*, 89(427):846–866, 1994.
- E. J. Oh, B. E. Shepherd, T. Lumley, and P. A. Shaw. Improved generalized raking estimators to address dependent covariate and failure-time outcome error. *Biometrical Journal*, 63(5):1006–1027, 2021a.
- E. J. Oh, B. E. Shepherd, T. Lumley, and P. A. Shaw. Raking and regression calibration: Methods to address bias from correlated covariate and time-to-event error. *Statistics in Medicine*, 40(3):631–649, 2021b.

- G. Amorim, R. Tao, S. Lotspeich, P. A. Shaw, T. Lumley, R. C. Patel, and B. E. Shepherd. Three-phase generalized raking and multiple imputation estimators to address error-prone data. *Statistics in Medicine*, 43(2):379–394, 2024.
- Jessie K. Edwards, Stephen R. Cole, Melissa A. Troester, and David B. Richardson. Accounting for misclassified outcomes in binary regression models using multiple imputation with internal validation data. *American Journal of Epidemiology*, 177(9):904–912, 2013.
- Stephen R Cole, Haitao Chu, and Sander Greenland. Multiple-imputation for measurement-error correction. *International Journal of Epidemiology*, 35(4):1074–1081, 2006.
- J. K. Edwards, S. R. Cole, D. Westreich, H. Crane, J. J. Eron, W. C. Mathews, R. Moore, S. L. Boswell, C. R. Lesko, M. J. Mugavero, and CNICS. Multiple imputation to account for measurement error in marginal structural models. *Epidemiology*, 26(5):645–652, 2015.
- J. K. Edwards, S. R. Cole, and M. P. Fox. Flexibly accounting for exposure misclassification with external validation data. *American Journal of Epidemiology*, 189(8):850–860, 2020.
- B. E. Shepherd, P. A. Shaw, and L. E. Dodd. Using audit information to adjust parameter estimates for data errors in clinical trials. *Clinical Trials*, 9(6):721–729, 2012.
- K. Han, P. A. Shaw, and T. Lumley. Combining multiple imputation with raking of weights: An efficient and robust approach in the setting of nearly true models. *Statistics in Medicine*, 40(30):6777–6791, 2021.
- I. Pelgrims, B. Devleeschauwer, S. Vandevijvere, E. M. De Clercq, S. Vansteelandt, V. Gorasso, and J. Van der Heyden. Using random-forest multiple imputation to address bias of self-reported anthropometric measures, hypertension and hypercholesterolemia in the Belgian health interview survey. *BMC Medical Research Methodology*, 23(1):69, 2023.
- United States Census Bureau. Centers of population. <https://www.census.gov/geographies/reference-files/time-series/geo/centers-population.html>, 2021. [Online; accessed 27-February-2024].
- R.W. Sinnott. Virtues of the haversine. *Sky and Telescope*, 68(2):159, 1984.
- Robert J. Hijmans. *geosphere: Spherical Trigonometry*, 2022. URL <https://CRAN.R-project.org/package=geosphere>. R package version 1.5-18.
- K. G. M. Moons, R. A. R. T. Donders, T. Stijnen, and F. E. Harrell. Using the outcome for imputation of missing predictor values was preferred. *Journal of Clinical Epidemiology*, 59(10):1092–1101, 2006.
- Lucy D’Agostino McGowan, Sarah C. Lotspeich, and Staci A. Hepler. The ‘Why’ behind including ‘Y’ in your imputation model. *Statistical Methods in Medical Research*, 2024. in press.
- Donald B Rubin. *Multiple imputation for nonresponse in surveys*, volume 81. John Wiley & Sons, 2004.
- Economic Research Service (ERS), U.S. Department of Agriculture (USDA). *Food Access Research Atlas*, 2019. <https://www.ers.usda.gov/data-products/food-access-research-atlas/>.
- M. White. Food access and obesity. *Obesity Reviews*, 8(Suppl. 1):99–107, 2007.
- Kyle Walker and Matt Herman. *tidycensus: Load US Census Boundary and Attribute Data as ‘tidyverse’ and ‘sf’-Ready Data Frames*, 2024. URL <https://CRAN.R-project.org/package=tidycensus>. R package version 1.6.3.
- Centers for Disease Control and Prevention. PLACES. <https://www.cdc.gov/places>, 2022. [Online; accessed 20-April-2023].
- Centers for Disease Control and Prevention. Methodology. <https://www.cdc.gov/places/methodology/index.html>, 2023. [Online; accessed 6-May-2024].
- United States Department of Agriculture. Historical SNAP Retailer Locator Data. <https://www.fns.usda.gov/snap/retailer/historicaldata>, 2022. [Online; accessed 21-July-2023].
- Edzer Pebesma and Roger S. Bivand. *Spatial Data Science With Applications in R*. Chapman & Hall, 2023. URL <https://r-spatial.org/book/>.
- L. A. Waller and C. A. Gotway. *Applied Spatial Statistics for Public Health Data*. Hoboken, N.J: John Wiley & Sons, 2004.
- François Rousset and Jean-Baptiste Ferdy. Testing environmental and genetic effects in the presence of spatial autocorrelation. *Ecography*, 37(8):781–790, 2014. URL <https://dx.doi.org/10.1111/ecog.00566>.
- Roderick J. A. Little. Regression with missing X’s: A review. *Journal of the American Statistical Association*, 87(420):1227–1237, 1992.
- L. Tang, R.H. Lyles, C.C. King, D.D. Celentano, and Y. Lo. Binary regression with differentially misclassified response and exposure variables. *Statistics in Medicine*, 34(9):1605–1620, 2015.

- Pamela A Shaw, Paul Gustafson, Raymond J Carroll, Veronika Deffner, Kevin W Dodd, Ruth H Keogh, Victor Kipnis, Janet A Tooze, Michael P Wallace, Helmut Küchenhoff, et al. STRATOS guidance document on measurement error and misclassification of variables in observational epidemiology: part 2—more complex methods of adjustment and advanced topics. *Statistics in medicine*, 39(16):2232–2263, 2020.
- Yanping Wang, Raymond H. Myers, Eric P. Smith, and Keying Ye. D-optimal designs for Poisson regression models. *Journal of Statistical Planning and Inference*, 136(8):2831–2845, 2006.
- G. Amorim, R. Tao, S. Lotspeich, P. A. Shaw, T. Lumley, and B. E. Shepherd. Two-phase sampling designs for data validation in settings with covariate measurement error and continuous outcome. *Journal of the Royal Statistical Society: Series A*, 184(4):1368–1389, 2021.
- S.C. Lotspeich, G.G.C. Amorim, P.A. Shaw, R. Tao, and B.E. Shepherd. Optimal multiwave validation of secondary use data with outcome and exposure misclassification. *Canadian Journal of Statistics*, 52:532–554, 2024.

Acknowledgements

The authors gratefully acknowledge the Andrew Sabin Family Center for Environment and Sustainability at Wake Forest University for a seed grant that supported this work.

Supplementary Materials

- **Additional appendices, tables, and figures:** The supplemental figures and tables referenced in Sections 2–5 are available online at https://github.com/sarahlotspeich/food_access_imputation/blob/main/Supplementary_Materials.pdf as Supplementary Materials.
- **R-package for imputation:** An R package `possum` that implements the multiple imputation methods described in this article is available at <https://github.com/sarahlotspeich/possum>.
- **R code and data for simulation studies and analysis:** The R scripts and data needed to replicate the simulation studies from Section 3 and data analysis from Section 4 are available at https://github.com/sarahlotspeich/food_access_imputation.